Effect of post-deposition solution treatment and ageing on improving interfacial adhesion strength of cold sprayed Ti6Al4V coatings

Boruah, D. & Zhang, X.

Original citation:
Boruah, D & Zhang, X 2021, 'Effect of post-deposition solution treatment and ageing on improving interfacial adhesion strength of cold sprayed Ti6Al4V coatings', Metals, vol. 11, no. 12, 2038.
https://dx.doi.org/10.3390/met11122038

DOI 10.3390/met11122038
ESSN 2075-4701

Publisher: MDPI

metals

MDPI

Article

Effect of Post-Deposition Solution Treatment and Ageing on Improving Interfacial Adhesion Strength of Cold Sprayed Ti6Al4V Coatings

Dibakor Boruah [1,2,*] and Xiang Zhang [1]

[1] Faculty of Engineering, Environment and Computing, Coventry University, Coventry CV1 5FB, UK; xiang.zhang@coventry.ac.uk
[2] Department of Electromechanical, Systems and Metal Engineering, Faculty of Engineering and Architecture, Ghent University, 9052 Gent, Belgium
* Correspondence: dibakor.boruah@ugent.be

Abstract: This study aims at investigating the effect of post-deposition solution treatment and ageing (STA) on improving the interfacial adhesion strength in cold spray (CS) Ti6Al4V coatings deposited on Ti6Al4V substrates, measured by the adhesive-free collar-pin pull-off (CPP) test. Solution treatment was performed at 940 °C for 1 h and ageing was carried out at 480 °C for 8 h. Investigations were carried out for specimens with three different pre-treatments of the substrate surface, namely grit-blasted, as-machined (faced on lathe machine), and ground. Additionally, the effect of post-deposition STA was studied in terms of phase analysis, microstructure, and porosity level. It was observed that STA led to complete interfacial mixing resulting in significantly improved adhesion strength (by more than 520%) with the maximum measured value of greater than 766 MPa for ground substrates, reaching 81% of the ultimate tensile strength of mill annealed Ti6Al4V.

Keywords: additive manufacturing; adhesion strength; coatings; cold spray; heat treatment; repairs; titanium alloy; Ti6Al4V

Citation: Boruah, D.; Zhang, X. Effect of Post-Deposition Solution Treatment and Ageing on Improving Interfacial Adhesion Strength of Cold Sprayed Ti6Al4V Coatings. *Metals* **2021**, *11*, 2038. https://doi.org/10.3390/met11122038

Academic Editor: Timothy John Eden

Received: 29 October 2021
Accepted: 8 December 2021
Published: 15 December 2021

1. Introduction

Titanium alloy Ti6Al4V is widely used in various industrial sectors with growing demand due to its well-known chemical, physical, and mechanical properties. Particularly in the aerospace sector, Ti6Al4V has diverse applications such as for engine parts, hydraulic tubbing, landing gear, load-bearing airframe structures, etc. [1,2]. However, these components are susceptible to various in-service damages including fatigue cracks, fretting/galling wear, etc. Generally, repair or remanufacturing is a more sustainable alternative to replacement, which has become more promising with the advancement of Cold Spray (CS) technology. In CS, a supersonic jet of preheated compressed gas (typically, N_2 and/or He) is used to propel the powder particles to reach a critical velocity. The high-velocity collision of the sprayed particles and accompanied plastic deformation result in deposited layers. The lower deposition temperature of the CS process is advantageous to minimize (or even eliminate) the detrimental effects associated with high-temperature processes such as oxidation, phase transformations, high tensile residual stresses, heat-affected zones, etc. [3].

The interfacial adhesion strength is the maximal normal stress needed to separate or detach a coating from its substrate, which is an imperative parameter for the structural integrity of CS deposits for load-bearing repair applications. For CS deposits, interfacial adhesion strength is a function of various process parameters, substrate surface preparation/roughness, coating thickness, etc. In the recent past, many researchers [1,4–15] have investigated the adhesion strength of CS Ti6Al4V deposited on Ti6Al4V substrates, focusing on different areas as listed in Table 1. Investigations were carried out using various

test standards/methods, such as the adhesive-based tensile adhesion test (TAT) as per ASTM C633 [4–9,11,12,14,15], and the portable adhesion test (PAT) as per ASTM D4541 [10]. However, conventional adhesive-based test methods are not suitable for measuring the adhesion strength of coatings when it exceeds the maximum limit (70–90 MPa) of typical adhesives used to bond the specimen parts. Therefore, a few studies have recently used adhesive-free methods such as the laser shock adhesion test (LASAT) [5], modified ASTM E8 [13,15], modified ASTM C633 [16,17], and collar-pin pull-off (CPP) test [1].

Table 1. Earlier studies reported the interfacial adhesion strength of CS Ti6Al4V deposited on Ti6Al4V substrates.

Area of Study	Variables Investigated	Gas, Pressure & Temperature (MPa, °C)	Test Methods	Authors (et al.)
Effect of CS process parameters	Working gas (N_2, He, N_2 + He mixtures), and particle velocity (700–855 m/s for N_2, 1200–1300 m/s for He)	N_2, He (5, 950)	ASTM C633	Khun [4]
		N_2 (4.5, 800–1000) N_2 + He (4.5, 1000)	ASTM C633	Tan [8]
	Process gas temperature (400 to 1000 °C)	N_2 (4.14, 400–500)	ASTM D4541	Bhattiprolu [10]
		N_2 (3, 550–750)	ASTM C633	Zhou [9]
		N_2 (4.5, 800–1000)	ASTM C633	Tan [8]
	Different feedstock powders, and nozzle length (120, 200 mm)	N_2 (4.14, 400–500)	ASTM D4541	Bhattiprolu [10]
	Gun traverse scanning speed (100 to 500 mm/s)	N_2 (4.5, 1000)	ASTM C633	Tan [11]
		N_2 (5, 1100)	Collar-Pin Pull-off	Boruah [1]
	Track spacing (1, 2 mm), and toolpath patterns (crosshatch, horizontal raster)	N_2 (5, 1100)	Collar-Pin Pull-off	Boruah [1]
Effect of substrate condition	Different substrate surface preparations or pre-treatments, and surface roughness (0.05 to 5.65 µm)	N_2 (4.5, 950)	ASTM C633	Tan [12]
		N_2 (4, 800)	ASTM C633	Costil [6]
		N_2 (4, 800)	ASTM C633, and LASAT	Perton [5]
		N_2 (5, 1100)	Collar-Pin Pull-off	Boruah [1]
Effect of coating thickness	Coating thickness (0.1 to 6 mm)	N_2 (4.8, 1100)	ASTM C633	Tan [15]
		N_2 (5, 1100)	Collar-Pin Pull-off	Boruah [1]
Effect of post-processing	Annealing at 600, 800, 1000 °C for 2 h	N_2 (2.5, 680)	ASTM C633	Zhou [14]
	Annealing at 600, 950 °C for 1 h	N_2 (4.5, 1000)	Modified ASTM E8	Bhowmik [13]
	Mechanical peening: deep cold rolling, controlled hammer peening	N_2 (5, 1000)	ASTM C633	Maharjan [7]

Khun et al. [4] studied the effect of process gases on the adhesion strength as per ASTM C633 [18]. They found that the CS Ti6Al4V coatings deposited with He possessed ~81% higher adhesion strength (75.1 MPa) than the coatings deposited with N_2 (41.4 MPa). Tan et al. [8] studied the influence of particle velocities on adhesion strength using ASTM C633. However, all specimens failed at the adhesive bond-line or with adhesive failure mode around 62–70 MPa. Zhou et al. [9] investigated the effect of in-situ shot peening assisted CS Ti6Al4V deposited at different temperatures (N_2, 550–750 °C) using ASTM C633 and found that bonding strength increased as the temperature increased, with the highest measured strength 36.5 MPa for specimens deposited at 750 °C. Bhattiprolu et al. [10] studied the influence of feedstock powder and process parameters using ASTM D4551 [19], and reported that hydride de-hydride powders showed comparable adhesion with plasma-atomized and gas-atomized powders. Moreover, increasing the nozzle length from 120 to 200 mm led to increased particle velocities for each powder type, resulted in higher adhesion strength (66–69 MPa) with adhesive failure. Tan et al. [11] investigated the effect of traverse scanning speeds (100–500 mm/s) using ASTM C633. They reported very low adhesion strength (~2.5 MPa with coating-substrate interface failure) for specimens

deposited at 100 mm/s scanning speed, and the specimens deposited at 300 and 500 mm/s had much higher adhesion strength of around 60–63 MPa with adhesive failure.

Tan et al. [12] studied the influence of substrate surface roughness (R_a, 0.05–5.4 μm) with four different substrate preparations using ASTM C633. A fall in adhesion strength was observed with the increase in substrate surface roughness. The highest reported strength was 69 MPa (adhesive failure) for polished substrate with R_a 0.05 μm. Costil et al. [6] reported similar results (around 80 MPa) with adhesive failure in most cases while attempting to study the influence of different surface pre-treatments on adhesion strength using ASTM C633. Perton et al. [5] further investigated the effect of various substrate pre-treatments/surface roughness finding that adhesion strength was higher when roughness values were either very high (5.53 μm) or very low (0.5, 0.12 μm), with the highest adhesion strength for mirror finished surface (i.e., the lowest roughness R_a 0.05 μm, >80 MPa from ASTM C633 with adhesive failure, and 900 MPa from LASAT).

The influence of coating thicknesses on the interfacial adhesion strength was investigated by Tan et al. [15], tests were performed as per ASTM C633. They reported that samples were failed with adhesive failure at around 65–70 MPa instead of the intended interface failure. Adhesive failure in the aforementioned investigations by various researchers [5,6,8,10–12,15] reveals that the coating adhesion strength of CS Ti6Al4V deposited on Ti6A4V substrate is greater than the typical tensile strength of adhesives used to bond the specimens according to conventional adhesive-based test methods. Consequently, Tan et al. [15] have developed an adhesive-free method (modified ASTM E8) for measuring true adhesion strength, which was reported as ~90 MPa with interface failure. Recently, Boruah et al. [1] performed a parametric study using the adhesive-free collar-pin pull-off (CPP) test to investigate the influence of various CS process variables (track spacing, scanning speed, and deposition toolpath pattern) and geometrical variables (coating thickness, and substrate surface preparations) on the interfacial adhesion strength. Two key findings are that the adhesion strength was 42% higher when deposited using cross-hatch toolpath pattern (91 MPa) when compared to horizontal raster (64 MPa), and the maximum strength was 122 MPa for ground substrates with R_a 0.58 μm (with adhesive failure for all CPP specimens) [1].

Regarding the effect of thermal treatments, Zhou et al. [14] studied the effect of annealing heat treatments (600–1000 °C for 2 h) on the in-situ shot peening assisted CS Ti6Al4V deposits using ASTM C633. They reported significant improvement in adhesion strength from 30 MPa (interface failure) in as-deposited condition to 54–58 MPa (adhesive failure) after annealing at 800–1000 °C for 2 h. Bhowmik et al. [13] also studied the effect of annealing treatments using the modified ASTM E8, and reported significant improvement in adhesion strength from 89 MPa (interface failure) in as-deposited condition to 747 MPa after annealing at 950 °C for 1 h (cohesion failure (i.e., failure within the CS deposited material)). Most recently, Maharajan et al. [7] investigated the effect of two mechanical peening methods (deep cold rolling, controlled hammer peening) using ASTM C633. They found that both peening methods improved adhesion strength, however, all peened specimens failed with adhesive failure and the true adhesion strength could not be determined.

Based on the literature on the adhesion strength on Ti6Al4V coatings deposited on Ti6Al4V substrates, it was observed that there has been much exploration in terms of the influence of process and geometrical variables. However, there is limited research on the effect of post-deposition thermal treatments on adhesion strength. Despite that, it is crucial to perform thermal treatments to improve adhesion strength along with other benefits such as microstructure homogenization, porosity reduction, residual stress relieving, and enhancing other mechanical properties. One of the main reasons behind the limited study on the effect of thermal treatments on adhesion strength could be the limitation of conventionally used adhesive-based methods. Adhesion strength is expected to be much higher after thermal treatments, which is beyond the upper limit of adhesive-based

methods (i.e., 70–90 MPa). According to the authors' best knowledge, no study has reported the influence of solution treatment and ageing (STA) treatment on the CS adhesion strength.

In this study, the adhesive-free collar-pin pull-off (CPP) test [1] was used to investigate the effect of STA treatment on the adhesion strength of CS Ti6Al4V coatings deposited on Ti6Al4V substrates with three substrate surface preparation conditions, namely (i) grit-blasted, (ii) as-machined, and (iii) ground. Additionally, cross-sections of the specimens were analyzed by means of phase identification, interface microstructure, and cross-sectional area fraction of porosity.

2. Experimental Methodology

2.1. Substrate Material and Feedstock Powder

The substrate material used was a mill annealed Ti6Al4V (grade 5) received from Dynamic Metals Ltd., Bedfordshire, UK. A commercially available gas-atomized Ti6Al4V powder (grade 5; size: d_{10} 17 µm, d_{50} 23 µm, d_{90} 32 µm) was used for cold spraying, supplied by LPW Technology Ltd., Cheshire, UK, as presented in Figure 1. Chemical compositions of the feedstock powder and substrate material can be found in [1,20].

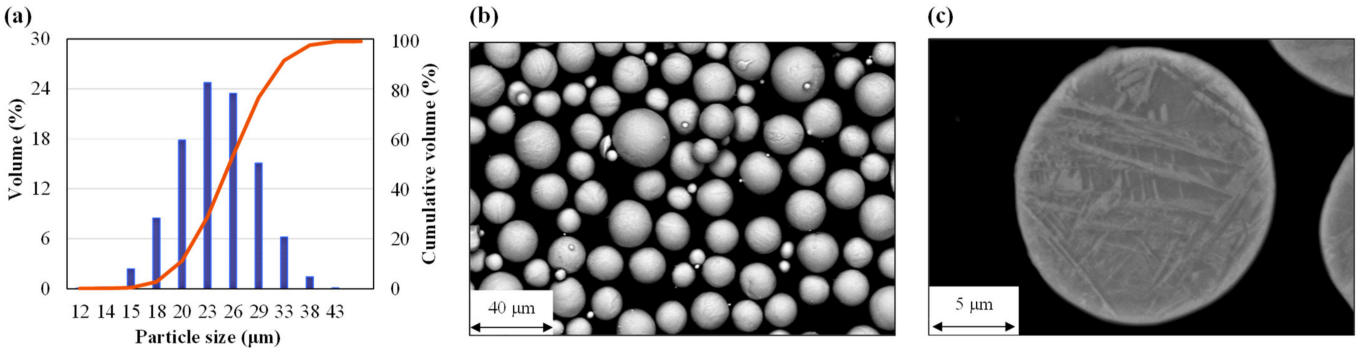

Figure 1. Characteristics of the gas-atomized Ti6Al4V powder: (**a**) size distribution, (**b**) morphology, and (**c**) microstructure [1,20].

2.2. Cold Spray Process Conditions and Specimen Preparation

All specimens were produced using a high-pressure CS system (Impact Innovation 5/11) installed at TWI Ltd., Cambridge, UK. The CS process variables used for depositing Ti6Al4V on Ti6Al4V substrates are shown in Table 2. Collar pin pull-off (CPP) test specimens were produced for three substrate surface pre-treatments viz. grit-blasted, as-machined, and ground, as listed in Table 3. Figure 2 shows 3D surface profilometry of test specimens with three different substrate surface preparations along with respective surface roughness (measured using Alicona InfiniteFocusSL as per ISO 4288 [21]). Solution treatment and ageing (STA) was performed under vacuum at 940 °C for 1 h followed by argon fast cooling and subsequent ageing at 480 °C for 8 h followed by furnace cooling to room temperature.

Table 2. Key process parameters used to deposit Ti6Al4V cold spray (CS) coatings on Ti6Al4V substrates.

Process gas	N_2
Process gas pressure (MPa)	5
Process gas temperature (°C)	1100
Powder feeding rate (g/min)	24.67
Traverse scanning speed (mm/s)	500
Track spacing or step size (mm)	2
Spraying angle (°)	90
Standoff distance (mm)	30
Deposition toolpath pattern	Horizontal raster

Table 3. Specimen details used for evaluating interfacial adhesion strength.

Specimen Type	Substrate Preparation	No. of CS Layers	Coating Thickness (mm)	Toolpath Pattern	Average Layer Thickness (µm)	No. of Specimens
CPP1 CPP2 CPP3	Grit-blasted [a] As-machined [b] Ground [c]	24	2.6	Horizontal raster	~107	3

[a] Grit-blasted using Tungsten Carbide (nominal size 44 µm) sprayed at an angle of 60° (Figure 2a); [b] As-machined i.e., faced on lathe machine (Figure 2b); [c] Ground with 320 alumina grit paper (Figure 2c).

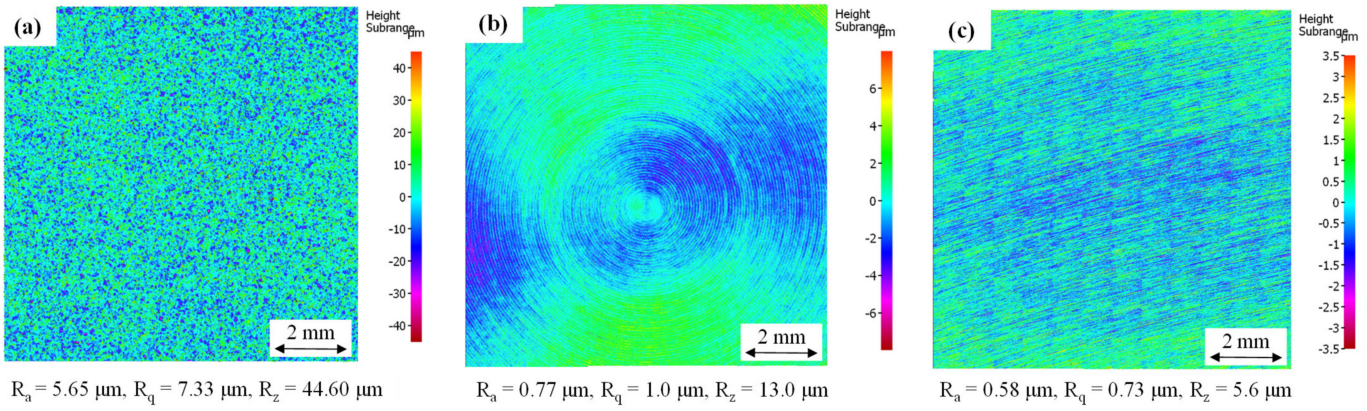

Figure 2. 3D surface profile measured by focus variation technique for different surface preparation conditions: (**a**) grit-blasted, (**b**) as-machined, and (**c**) ground (adopted from [1]).

2.3. Collar-Pin Pull-Off (CPP) Test Method

To measure interfacial adhesion strength, the collar-pin pull-off (CPP) test [1] was used. The CPP test is an adhesive-free method comprising a 'pin' and a 'collar' assembled with two grub screws. The original idea of the CPP test was taken from the designs published in [22,23], which was further modified/improved for easy integration with ASTM C633 [18] test fixtures. The specimen preparation process and the schematic of the CPP test set-up are shown in Figure 3, further details of the test method can be found in [1]. All tests were conducted under displacement control mode using Instron 8801 (50 kN).

2.4. Cross-Sectional Analysis: Phase Identification and Microstructure

The phase information was examined using X-ray diffractometer or XRD (Bruker' s D8 Advance, Billerica, MA, USA). Measurements were performed from 20° to 90° of 2θ using a Cu Kα radiation source with wavelength, λ = 1.5406 Å. The purpose was to compare the XRD patterns of Ti6Al4V material in different conditions: gas atomized feedstock power, mill annealed substrate, CS as-deposited, and CS deposits after STA.

For the microstructural study, samples were cross-sectioned (parallel to the build direction). Afterwards, they were prepared using standard metallographic procedures, which includes cold mounting, manual grinding with SiC abrasive paper discs (up to grit size 2500), followed by automatic polishing with OP-U colloidal silica. Specimens were etched using Kroll' s reagent for 10–15 s. To examine microstructures of the etched and polished samples, optical microscope (Olympus BX41M-LED, Tokyo, Japan) and scanning electron microscope or SEM (ZEISS EVO LS 15, Jena, Germany) were used. SEM images were taken using the backscatter electron detector (BSE) mode. For porosity measurement, a minimum of 20 continuous cross-sectional micrographs was taken at 10× magnification. Porosity measurements were performed as per ASTM E2109 [24], and the ImageJ software was used to locate pores and to calculate the two-dimensional area fraction of porosity (%). All images were converted to 8-bit and a suitable threshold was created for porosity analysis.

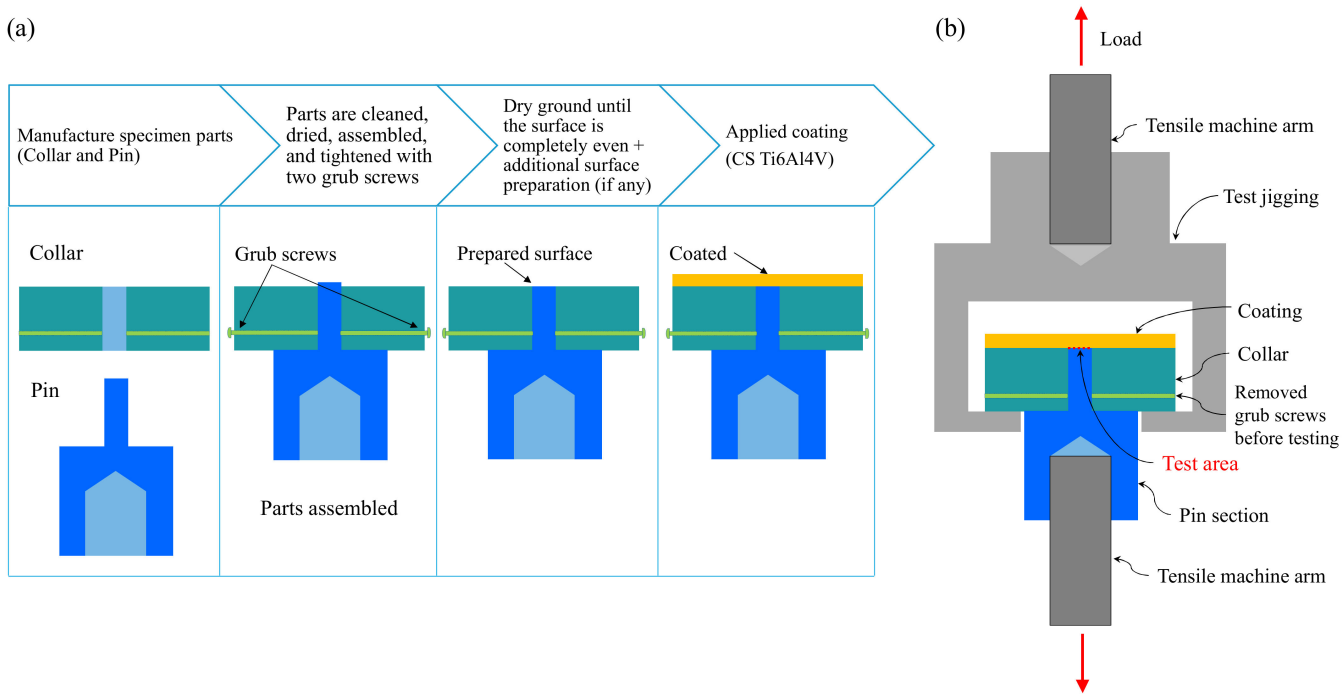

Figure 3. The adhesive-free collar-pin pull-off (CPP) test method: (**a**) specimen preparation process, (**b**) experimental set-up [1].

3. Results

3.1. Interfacial Adhesion Strength

Interfacial adhesion strength results for all investigated conditions are shown in Figure 4a,b, representing a significant improvement in adhesion strength in CS Ti6Al4V coatings deposited on Ti6Al4V substrates as a result of the post-deposition STA process. Figure 4a shows stress vs. displacement curves (one example for each condition) derived from load vs. displacement data from CPP tests, and Figure 4b presents average adhesion strength (calculated from the maximum load at failure) for six different investigated conditions. For grit-blasted substrate with relatively high surface roughness (R_a 5.65 µm), adhesion strength improved by around 222% (i.e., from 82 MPa in the AD condition to 264 MPa after STA). Strikingly, for substrates with low surface roughness (as-machined: R_a 0.77 µm, ground: R_a 0.58 µm), a significant improvement in adhesion strength by more than 520% was achieved after STA (i.e., from 112 MPa to above 726 MPa for the as-machined substrate, and from 122 MPa to above 766 MPa for the ground substrate). The failure mode of all specimens in AD condition was interface failure. After STA, specimens with grit-blasted substrate failed with interface failure mode, but specimens with as-machined and ground having very high adhesion strength failed with cohesion failure mode.

Images of STA treated CPP test specimens with three different substrate pre-treatments and their respective failure modes are presented in Figure 5a, displaying interface failure mode for the samples with grit-blasted substrate surfaces, and cohesion failure mode for the as-machined and the ground substrate surfaces. A close-up of the 'pin' with CS deposits adhered to it can be seen in Figure 5b after the cohesion failure. Initially, it was speculated that there might be metallurgical bonding at the sidewall between the 'pin' and the 'collar' after the STA process, and that might have influenced the adhesion strength results. Therefore, surfaces of the 'pin' sidewalls of the tested CPP samples were examined under SEM, but, no indication of metallurgical bonding was evident between the collar and pin's sidewall surface. SEM micrographs of the pin's sidewall surface (after STA) in two different magnifications are presented in Figure 5b.

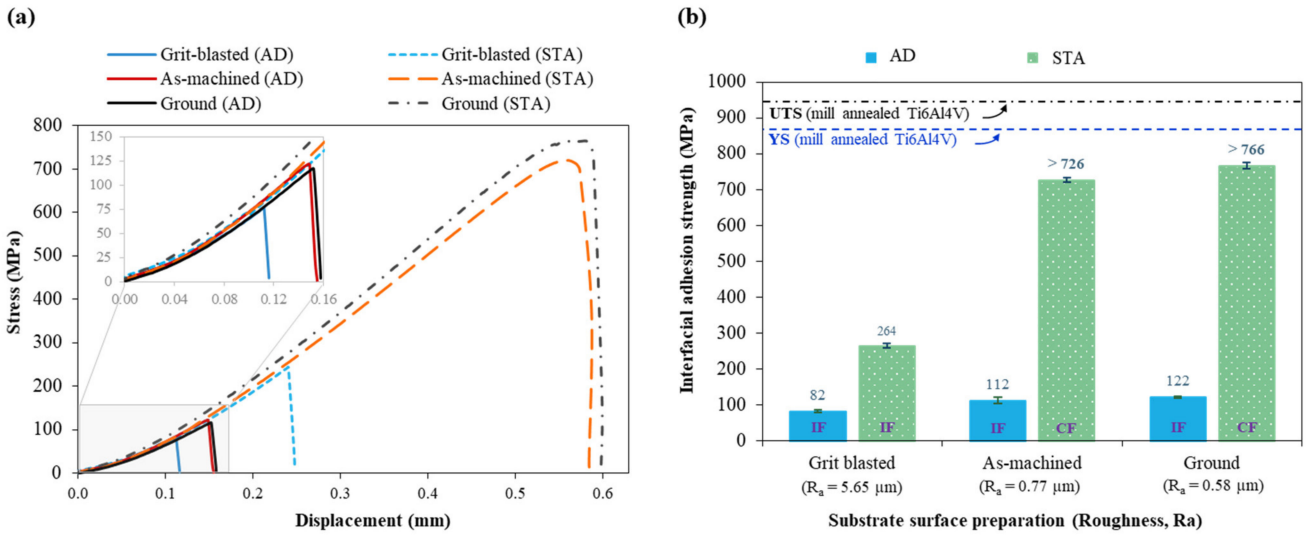

Figure 4. Effect of STA on the interfacial adhesion strength for different substrate surface preparations: (**a**) stress vs. displacement curve, showing one example for each condition; (**b**) interfacial adhesion strength (average of three tests). (Note: AD-As-deposited, STA-Solution Treated and Aged, IF-Interface Failure, CF-Cohesion Failure).

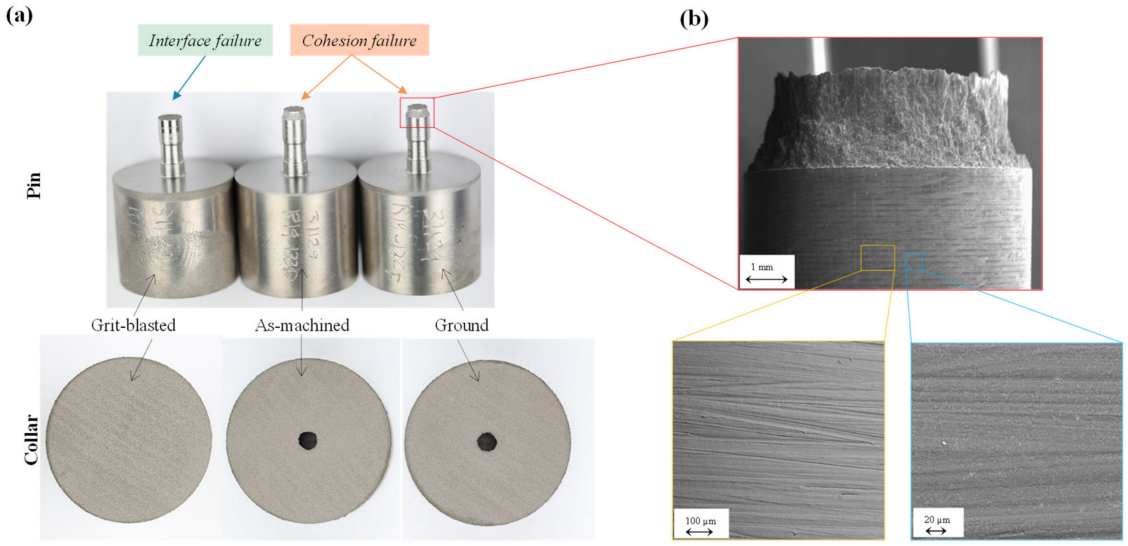

Figure 5. Tested collar-pin pull-off (CPP) specimens: (**a**) failure mechanisms showing interface failure and cohesion failure, (**b**) an enlarged view of the 'pin' with cohesion failure, and further magnified images of its sidewall surface showing no evidence of metallurgical bonding between the 'collar' and 'pin' sidewall surface after STA treatment.

3.2. Phase Analysis and Microstructure of the Cross-Section

XRD patterns shown in Figure 6 reveal dominant α-Ti peaks with no evident traces of β-Ti for CS as-deposited samples, which is comparable to the feedstock powder. XRD patterns showed no impurities, no additional phases or apparent phase transformation and that no oxidation happened during cold spraying as well as in the STA process. However, for as-deposited CS Ti6Al4V, obvious peak shifts/broadening can be observed when compared to feedstock powder. Particularly, the peak intensity of {0002} plane was higher, which could be due to the severe deformation of the Ti6Al4V particles indicating the formation of refined crystals and microstructure [25,26].

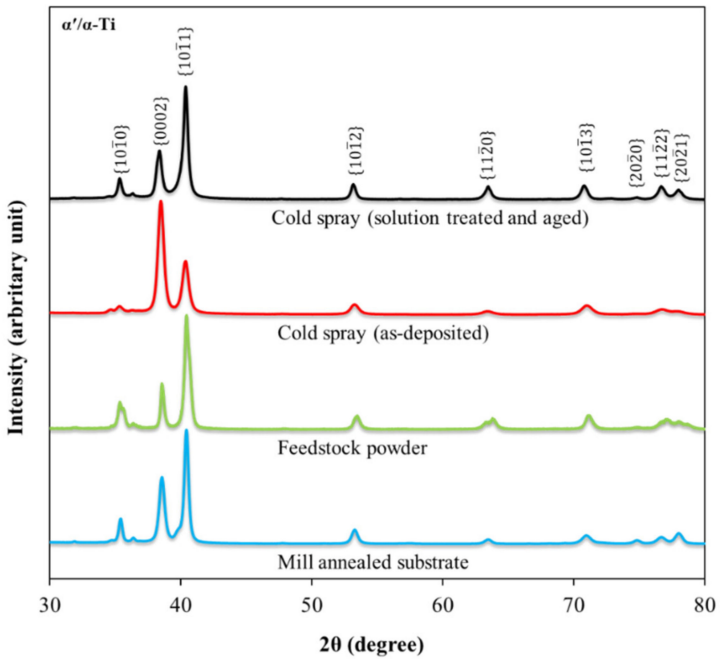

Figure 6. XRD patterns of Ti6Al4V in the sample cross-section covering various materials: mill annealed substrate, feedstock powder, cold spray deposits (as-deposited, solution treated, and aged).

The etched cross-sectional microstructures of the coating-substrate interfaces with three different substrate surface preparation conditions are presented in Figure 7, both before and after STA for comparison. In the AD condition, the microstructure of CS deposits is generally comprised of partially deformed 'textured' regions and severely deformed 'smooth' regions inherited from the feedstock powder, whereas, the mesostructure is comprised of flattened powder particles that undergone severe plastic deformation with $2.25 \pm 0.16\%$ area fraction of porosity. STA led to complete disappearance of the microstructural features of the AD condition through nucleation and growth of recrystallized grains, which resulted in coarsened microstructure with equiaxed α grains (dark colored regions) with intergranular vanadium rich β precipitates (light colored regions) as shown in SEM images Figure 7c,f,i. Moreover, STA led to a reduction in porosity to $1.74 \pm 0.10\%$ as a result of solid-state densification through atomic thermal diffusion and grain boundary migration at the inter-particle contact interfaces. The same phenomenon also brings significant growth in metallurgical bonding via enhanced long-range diffusion at a higher temperature [13]. Nevertheless, remnants from grit-blasted particles can be seen in the interface for grit basted surfaces as can be observed in Figure 7a–c. In Figure 7h,i, the grain size of the ground substrate material appears to be smaller, although CS deposition process parameters and STA parameters were the same for all specimens. Therefore, it might be the case that substrate material (i.e., the 'Collar' part of CPP specimen) used for ground specimens came from a different batch of Ti6Al4V round bar or from different ends/regions of the same bar where the microstructure was slightly different.

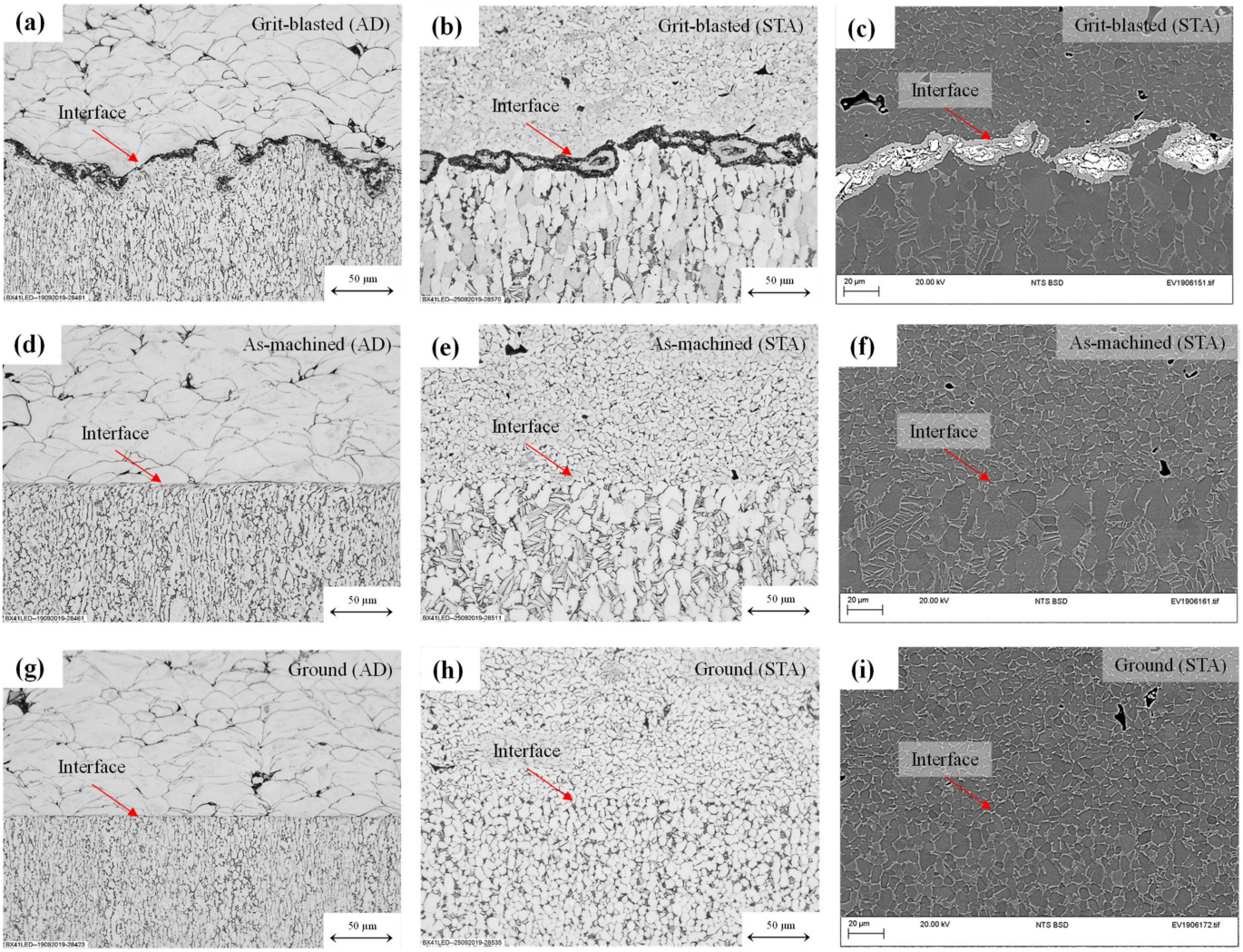

Figure 7. Cross-section microstructure images of the CS Ti6Al4V deposit/substrate interface, in as-deposited (AD) and solution treatment and aged (STA) conditions, with three different surface preparation conditions: (**a**–**c**) grit-blasted, (**d**–**f**) as-machined, (**g**–**i**) ground (of which (**a**,**b**,**d**,**e**,**g**,**h**) are optical micrographs), and (**c**,**f**,**i**) are SEM images. (**a**,**d**,**g**) are adopted from [1].

4. Discussion

Measuring interfacial adhesion strength in high strength coatings is one of the common challenges in the cold spray and thermal spray community, which is becoming more crucial due to the growing applications of CS in structural repairs that require load-bearing capacity. Recent development in adhesive-free methods [1,13,15–17] allows measurements of adhesion strength beyond the upper limit (i.e., around 90 MPa) of the conventionally used adhesive-based methods. The development of adhesive-free methods also permits investigation of unexplored topics (particularly for high strength coatings), such as parametric studies on the effect of process parameters, coating thicknesses, substrate-surface preparations [1], and thermal treatments [13]. Although adhesive-free methods possess certain advantages over conventional adhesive-based methods, there are also limitations. For example, adhesive-free methods based on [13,15–17] require a much thicker coating (~5 mm) and post-deposition machining to get desired dimensions. Coatings with such a high thickness induce high residual stresses and may cause interfacial cracks or delamination [11,20,27,28]. Moreover, post-deposition machining of the test specimens itself can be a challenge, especially for the CS deposited Ti alloys which is generally very hard and brittle. Furthermore, adhesion test results from thick coatings (~5 mm) are not representative of a

significantly thinner coating in application. On the other hand, the adhesive-free CPP test method [1] has some advantages, for example, it can be used for parametric studies such as to study the effect of coating thicknesses on adhesion strength. However, it can be argued that the cross-sectional area being tested in the CPP method is very localized (with a 5 mm pin diameter), making the results sensitive to any local defects or imperfections, which may not be representative of the average strength. Nevertheless, increasing the pin diameter is not a solution, as it significantly increases the non-uniformity in stress distribution along the interface leading to premature failure. Therefore a 5 mm pin diameter is a balance between these two factors [1]. Anyhow, it was found that the scatter in test results coming from the CPP test method is reasonably low (±5 MPa, average from this study and [1]) and comparable to scatter in ASTM C633 (±4 MPa, average from [4–6,8,9,11,12,14,15]).

In this study, the CPP test method is used for the first time to investigate the influence of post-deposition STA on the improvement in interfacial adhesion strength. The results reported in Section 3.1 showed that STA led to considerable improvement in interfacial adhesion strength (by more than 547% for as-machined surface, and by more than 527% for ground substrate) from its AD condition. The highest adhesion strength was measured for ground substrate as 766 MPa, but with cohesion failure, which means true adhesion strength can be higher than the measured value. This also represents that the adhesion strength is at least 81% of the ultimate tensile strength (~950 MPa) and 87% of the yield strength (~880 MPa) of mill annealed Ti6Al4V [29]. Recently, Bhowmik et al. [13] have also reported similar results with significant improvement in adhesion strength by more than 739% (i.e., from 89 MPa in the AD condition to >747 MPa after annealing at 950 °C for 1 h), measured using the modified ASTM E8. Table 4 compares the adhesion strength results of this study with the existing literature. Figure 8 represents the same adhesion strength results (before and after post-deposition thermal treatments) in terms of % of mill annealed Ti6Al4V' s ultimate tensile strength. In the case of 'cohesion failure' mode, a greater-than (>) symbol is being used while reporting the adhesion strength values, which indicates that the true value could be greater than the measured value.

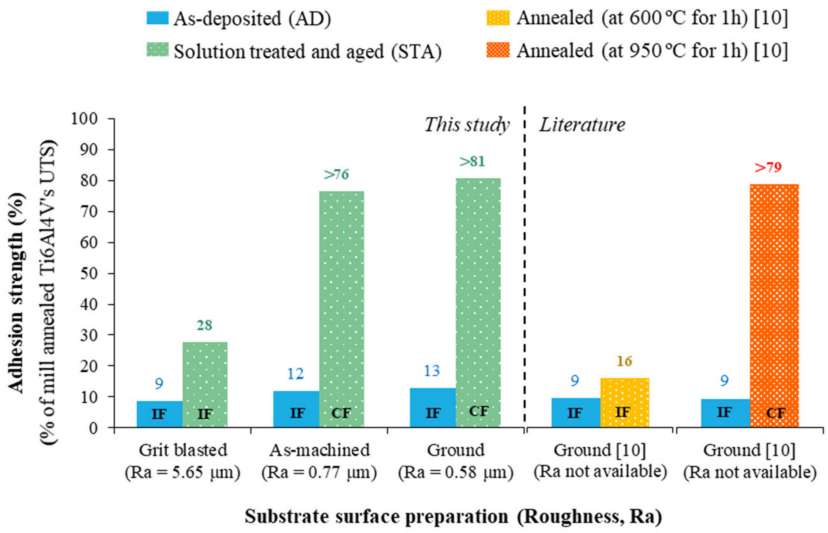

Figure 8. Adhesion strength in terms of % of mill annealed Ti6Al4V' s ultimate tensile strength (UTS), before and after thermal treatments, and comparison with the literature. (Note: IF-Interface Failure, and CF-Cohesion Failure).

Table 4. Effect of post-deposition thermal treatments on the adhesion strength of CS Ti6Al4V deposited on Ti6Al4V substrate: literature versus this study.

Gas (MPa, °C)	Scanning Speed (mm/s)	Stand-Off Distance (mm)	Coating Thickness (mm)	Substrate Surface Preparation	Testing Condition	Adhesion Strength (MPa), Failure Mechanism	Test Methods	Authors (et al.)
N_2, (2.5, 680)	100	20	0.3	Grit-blasted	As-deposited	30 ± 3, NA	ASTM C633	Zhou [14]
					Annealing at 600 °C for 2 h	34 ± 10, NA		
					Annealing at 800 °C for 2 h	54 ± 7, AF		
					Annealing at 1000 °C for 2 h	58 ± 4, AF		
N_2, (4.5, 1000)	500	30	4.5	Ground	As-deposited	~89, IF	Modified ASTM E8	Bhowmik [13]
					Annealing at 600 °C for 1 h	~152, IF		
					Annealing at 950 °C for 1 h	>747, CF		
N_2 (5, 1100)	500	30	2.6	Grit-blasted	As-deposited	82 ± 4, IF	Collar-Pin Pull-off (CPP)	Boruah [1]; This study
					STA	264 ± 6, IF		
				As-machined	As-deposited	112 ± 9, IF		
					STA	>726 ± 7, CF		
				Ground	As-deposited	122 ± 3, IF		
					STA	>766 ± 8, CF		

AF, adessive failure (i.e., failure at the adhesive bond line); CF, cohesion failure (i.e., failure within the CS deposits); IF, interface failure (i.e., failure at the coating substrate interface, also known as adhesion failure); NA, not available; STA, solution treated and aged (940 °C for 1 h and ageing at 480 °C for 8 h).

From the micrographs shown in Figures 4 and 6, it is obvious that the improvement in adhesion strength after STA was largely due to the enhanced metallurgical bonding at the interface. Particularly, for as-machined and ground substrate surface conditions, STA led to significant growth in metallurgical bonding at the interface resulting in complete interfacial mixing (interfaces are almost non-existent) and hence remarkably high adhesion strength. For grit-blasted substrate, a marginal increase in interfacial adhesion strength after STA could be due to embedded grit on the substrate (or remnants from grit-blasted particles) causing a barrier to grow interfacial metallurgical bonding between the substrate and the deposited particles.

Through-thickness residual stress profile measured in [3] using the neutron diffraction technique showed that STA resulted in complete relaxation of process-induced residual stresses. The relaxation of residual stresses after STA might have some contribution towards the significant improvement in adhesion strength, though it was believed to be predominantly due to the microstructural changes. As reported in [13], there were significant changes in microstructural features with a clear trend in the growth of metallurgical bonding with the increase in annealing temperatures (300, 400, 600 and 950 °C). However, the trend in the evolution of residual stresses with the increase in annealing temperatures was ambiguous. Annealing at both 600 and 950 °C relaxed residual stresses by almost the same amount, but the adhesion strength was improved from 89 MPa in the AD condition to 152 MPa after annealing at 600 °C, and to >747 MPa after annealing at 950 °C [13]. Therefore, it must be the microstructural changes (growth of metallurgical bonding) that improved interfacial adhesion strength rather than a relaxation of residual stresses after thermal treatments. Nonetheless, further investigation is required for a better understanding of the relative contribution of 'microstructural changes' and 'residual stress relaxation' to the interfacial adhesion strength after thermal treatments.

5. Conclusions

This study investigated the effect of solution treatment and ageing (STA) on the interfacial adhesion strength of cold spray (CS) deposited Ti6Al4V on Ti6Al4V substrates. Measurements were carried out using the adhesive-free collar-pin pull-off (CPP) test for specimens with three different substrate surface preparation conditions (grit-blasted, as-machined, and ground). In addition, cross-sections of deposit-substrate assemblies were analyzed in terms of X-ray diffraction (XRD), interfacial microstructure, and porosity level before and after STA. The following conclusions are drawn based on this research:

- The post-deposition STA has led to complete interfacial mixing, resulting in significantly improved adhesion strength by more than 520% compared to the as-deposited condition for both ground (R_a = 0.58 μm) and as-machined substrates (Ra = 0.77 μm). The maximum adhesion strength measured after STA was greater than 766 MPa for ground substrates (vs. 122 MPa in as-deposited condition), reaching 81% of the ultimate tensile strength of mill annealed Ti6Al4V. After STA, the cohesion failure mode was observed for both ground and as-machined substrates, indicating that the true adhesion strength could be higher than the measured value.
- No appreciable improvement in adhesion strength was observed for grit-blasted surfaces (Ra = 5.65 μm). In this case, STA improved adhesion strength by around 220%, from 82 MPa in the as-deposited (AD) condition to 264 MPa after STA (with interface failure mode). This might be due to the embedded impurities in the interface (remnants from grit-blasted particles) acting as a barrier to grow interfacial metallurgical bonding during the STA process.
- The relative study on cross-sectional area fraction of porosity showed a reduction in porosity after STA (2.25 ± 0.16% in the AD condition to 1.74 ± 0.10% post STA). The XRD patterns did not reveal any significant phase transformation as a result of STA.
- Using the CPP test allowed for measurement of the interfacial adhesion strength of Ti6Al4V coatings, particularly after STA, which is considerably higher than the upper limit (i.e., around 90 MPa) of conventional adhesive-based methods (for instance,

ASTM C633 or ASTM D4541). Notably, the tests performed after STA using the CPP method shows comparable results with the literature (measured by another adhesive-free test method, namely modified ASTM E8) for annealed specimens at temperatures close to solution treatment.

Author Contributions: Conceptualization, D.B. and X.Z.; formal analysis, D.B.; investigation, D.B.; methodology, D.B.; data curation, D.B.; writing—original draft preparation, D.B.; writing—review and editing, D.B. and X.Z.; visualization, D.B.; supervision, X.Z.; funding acquisition, X.Z. All authors have read and agreed to the published version of the manuscript.

Funding: This work was supported by Lloyd's Register Foundation under the Grant number DB012017COV; and Coventry University under the grant number 7486157.

Institutional Review Board Statement: Not applicable.

Informed Consent Statement: Not applicable.

Acknowledgments: This research was enabled through and undertaken at the National Structural Integrity Research Centre (NSIRC), a postgraduate engineering facility for industry-led research into structural integrity established and managed by TWI Ltd. This work was sponsored by the Lloyd' s Register Foundation (LRF), a charitable organization that helps to protect life and property by supporting engineering-related education, public engagement and the application of research. Authors would like to thank Abdul Khadar Syed, and Gowtham Soundarapandiyan at Coventry University, Matthew Dore, Ben Robinson, Philip McNutt, Henry Begg, and Raja Khan at TWI Ltd. for their technical and/or managerial support in various stages of this project.

Conflicts of Interest: The authors declare no conflict of interest. The funders had no role in the design of the study; in the collection, analyses, or interpretation of data; in the writing of the manuscript; or in the decision to publish the results.

References

1. Boruah, D.; Robinson, B.; London, T.; Wu, H.; de Villiers-Lovelock, H.; McNutt, P.; Doré, M.; Zhang, X. Experimental evaluation of interfacial adhesion strength of cold sprayed Ti-6Al-4V thick coatings using an adhesive-free test method. *Surf. Coat. Technol.* **2020**, *381*, 125130. [CrossRef]
2. Boyer, R.R. An overview on the use of titanium in the aerospace industry. *Mater. Sci. Eng. A* **1996**, *213*, 103–114. [CrossRef]
3. Boruah, D. Structural Integrity Assessment of Cold Spray Additive Manufactured Titanium Alloy Ti-6Al-4V. Ph.D. Thesis, Coventry University, Coventry, UK, 2020.
4. Khun, N.W.; Tan, A.W.Y.; Bi, K.J.W.; Liu, E. Effects of working gas on wear and corrosion resistances of cold sprayed Ti-6Al-4V coatings. *Surf. Coat. Technol.* **2016**, *302*, 1–12. [CrossRef]
5. Perton, M.; Costil, S.; Wong, W.; Poirier, D.; Irissou, E.; Legoux, J.G.; Blouin, A.; Yue, S. Effect of pulsed laser ablation and continuous laser heating on the adhesion and cohesion of cold sprayed Ti-6Al-4V coatings. *J. Therm. Spray Technol.* **2012**, *21*, 1322–1333. [CrossRef]
6. Costil, S.; Danlos, Y.; Wong, W. *The PROTAL ®Process Applied on Cold Spraying to Improve Interface Adherence and Coating Cohesion—Case of Titanium and Nickel Based Alloys*; Therm. Spray 2010 Glob. Solut. Future Appl.; National Research Council Publications: Ottawa, ON, Canada, 2010; pp. 836–841.
7. Maharjan, N.; Bhowmik, A.; Kum, C.; Hu, J.; Yang, Y.; Zhou, W. Post-processing of cold sprayed Ti-6Al-4V coatings by mechanical peening. *Metals* **2021**, *11*, 1038. [CrossRef]
8. Tan, A.; Lek, J.; Sun, W.; Bhowmik, A.; Marinescu, I.; Song, X.; Zhai, W.; Li, F.; Dong, Z.; Boothroyd, C.; et al. Influence of particle velocity when propelled using N2 or N2-He mixed gas on the properties of cold-sprayed Ti6Al4V coatings. *Coatings* **2018**, *8*, 327. [CrossRef]
9. Zhou, H.; Li, C.; Ji, G.; Fu, S.; Yang, H.; Luo, X.; Yang, G.; Li, C. Local microstructure inhomogeneity and gas temperature effect in in-situ shot-peening assisted cold-sprayed Ti-6Al-4V coating. *J. Alloys Compd.* **2018**, *766*, 694–704. [CrossRef]
10. Bhattiprolu, V.S.; Johnson, K.W.; Ozdemir, O.C.; Crawford, G.A. Influence of feedstock powder and cold spray processing parameters on microstructure and mechanical properties of Ti-6Al-4V cold spray depositions. *Surf. Coat. Technol.* **2018**, *335*, 1–12. [CrossRef]
11. Tan, A.W.Y.; Sun, W.; Phang, Y.P.; Dai, M.; Marinescu, I.; Dong, Z.; Liu, E. Effects of traverse scanning speed of spray nozzle on the microstructure and mechanical properties of cold-sprayed Ti6Al4V coatings. *J. Therm. Spray Technol.* **2017**, *26*, 1484–1497. [CrossRef]
12. Tan, A.W.Y.; Sun, W.; Bhowmik, A.; Lek, J.Y.; Song, X.; Zhai, W.; Zheng, H.; Li, F.; Marinescu, I.; Dong, Z.; et al. Effect of substrate surface roughness on microstructure and mechanical properties of cold-sprayed Ti6Al4V coatings on Ti6Al4V Substrates. *J. Therm. Spray Technol.* **2019**, *28*, 1959–1973. [CrossRef]

13. Bhowmik, A.; Tan, A.W.; Sun, W.; Wei, Z.; Marinescu, I. On the heat-treatment induced evolution of residual stress and remarkable enhancement of adhesion strength of cold sprayed Ti-6Al-4V coatings. *Results Mater.* **2020**, *7*, 100119. [CrossRef]
14. Zhou, H.; Li, C.; Luo, X.; Yang, G.; Hussain, T.; Li, C. Microstructure of cross-linked high densification network and strengthening mechanism in cold-sprayed Ti-6Al-4V coating after heat treatment. *J. Therm. Spray Technol.* **2020**, *29*, 1054–1069. [CrossRef]
15. Tan, A.W.Y.; Sun, W.; Bhowmik, A.; Lek, J.Y.; Marinescu, I.; Li, F.; Khun, N.W.; Dong, Z.; Liu, E. Effect of coating thickness on microstructure, mechanical properties and fracture behaviour of cold sprayed Ti6Al4V coatings on Ti6Al4V substrates. *Surf. Coat. Technol.* **2018**, *349*, 303–317. [CrossRef]
16. Huang, R.; Ma, W.; Fukanuma, H. Development of ultra-strong adhesive strength coatings using cold spray. *Surf. Coat. Technol.* **2014**, *258*, 832–841. [CrossRef]
17. Huang, R.; Fukanuma, H. Study of the influence of particle velocity on adhesive strength of cold spray deposits. *J. Therm. Spray Technol.* **2012**, *21*, 541–549. [CrossRef]
18. ASTM C633-13. *Standard Test Method for Adhesion or Cohesion Strength of Thermal Spray Coatings*; ASTM Int.: West Conshohocken, PA, USA, 2017.
19. ASTM D4541-17. *Standard Test Method for Pull-Off Strength of Coatings Using Portable Adhesion Testers*; ASTM Int.: West Conshohocken, PA, USA, 2017.
20. Boruah, D.; Ahmad, B.; Lee, T.L.; Kabra, S.; Syed, A.K.; McNutt, P.; Doré, M.; Zhang, X. Evaluation of residual stresses induced by cold spraying of Ti-6Al-4V on Ti-6Al-4V substrates. *Surf. Coat. Technol.* **2019**, *374*, 591–602. [CrossRef]
21. *ISO 4288:1996—Geometrical Product Specifications (GPS)—Surface Texture: Profile Method—Rules and Procedures for the Assessment of Surface Texture*; ISO: Geneva, Switzerland, 1996.
22. Sharivker, S.Y. Strength of adhesion of plasma sprayed coatings to the base material. *Sov. Powder Metall. Met. Ceram.* **1967**, *6*, 483–485. [CrossRef]
23. Lyashenko, B.; Rishin, V.; Zil'berberg, V.; Sharivker, S. Strength of adhesion between plasma-sprayed coatings and the base metal. *Sov. Powder Metall. Met. Ceram.* **1969**, *8*, 331–334. [CrossRef]
24. ASTM E2109—01. *Standard Test Methods for Determining Area Percentage Porosity in Thermal Sprayed Coatings*; ASTM Int.: West Conshohocken, PA, USA, 2014.
25. Sun, W.; Tan, A.W.Y.; Khun, N.W.; Marinescu, I.; Liu, E. Effect of substrate surface condition on fatigue behavior of cold sprayed Ti6Al4V coatings. *Surf. Coat. Technol.* **2017**, *320*, 452–457. [CrossRef]
26. Chen, C.; Xie, Y.; Yan, X.; Yin, S.; Huang, R.; Zhao, R.; Wang, J.; Ren, Z.; Liu, M.; Liao, H. Effect of hot isostatic pressing (HIP) on microstructure and mechanical properties of Ti6Al4V alloy fabricated by cold spray additive manufacturing. *Addit. Manuf.* **2019**, *27*, 595–605. [CrossRef]
27. Greving, D.J.; Shadley, J.R.; Rybicki, E.F.; Greving, D.J.; Shadley, J.R.; Rybicki, E.F. Effects of coating thickness and residual stresses on the bond strength of ASTM C633-79 thermal spray coating test specimens. *J. Therm. Spray Technol.* **1994**, *3*, 371–378. [CrossRef]
28. Boruah, D.; Zhang, X.; Doré, M. Theoretical prediction of residual stresses induced by cold spray with experimental validation. *Multidiscip. Modeling Mater. Struct.* **2019**, *15*, 599–616. [CrossRef]
29. ASM Material Data Sheet: Titanium Ti-6Al-4V (Grade 5), (n.d.). Available online: http://asm.matweb.com/search/SpecificMaterial.asp?bassnum=mtp641 (accessed on 27 July 2021).